M.D. Binder (Ed.)
Progress in Brain Research, Vol 123

CHAPTER 11

Quantifying proprioception

Arthur Prochazka*

Division of Neuroscience, University of Alberta, Edmonton, AB T6G 2S2, Canada

Introduction

The papers of Douglas Stuart and his colleagues in the 1970s on the properties of neuronal ensembles controlling cat locomotion (e.g. Goslow et al., 1973b; Wetzel and Stuart, 1976; Rasmussen et al., 1978), were among the most influential of their era. They heralded a transition from studies of segmental reflexes in immobile, anesthetized animals, to those in which ensembles of sensorimotor neurons controlling complex movements in awake animals are identified and characterized. The two papers on kinematic, EMG and proprioceptive responses during locomotion (Goslow et al., 1973a, b) have become classic references for all research laboratories concerned with the neural control of locomotion.

Jasper et al. (1958) and Evarts (1964) pioneered the recording of the activity of single neurons in the brain during motor behavior in awake monkeys. This had a tremendous impact on motor control and spawned many other studies and new approaches. Within a decade, techniques were developed for recording from single sensory afferent neurons in the dorsal root ganglia of freely-moving cats (Prochazka et al., 1976; Loeb et al., 1977). In a parallel development, Hagbarth and Vallbo (1967) pioneered the technique of human miocroneurography, which for the first time revealed the firing of single sensory axons in human peripheral nerves. This technique, which also had a major impact on the field, has the advantage that sensory activity is monitored in awake humans performing voluntary motor tasks, but it has the disadvantage that movement is greatly restricted in range and velocity because the microelectrodes are easily dislodged from the nerve.

Over the years, a consistent and puzzling difference emerged in the firing properties of human and animal muscle spindle afferents. In humans, spindle firing rates rarely exceeded 30 impulses/s, whereas in cats and monkeys performing motor tasks, the firing rate of spindle primary (Ia) afferents typically fluctuated between 25 and 200 impulses/s, transiently exceeding 500 impulses/s in demanding situations (review: Prochazka, 1996). Human neurographers have suggested that the difference in firing rates is due to a fundamental species difference. But my group has argued that it may be due merely to the large differences in muscle velocities in the human and animal experiments. The question is quite important from a control systems point of view and as we shall see, it is also relevant to another discrepancy, namely that in cats, fusimotor action appears to fluctuate dramatically with task and context (fusimotor 'set'), whereas in humans it seems to be exclusively linked to α-motoneuronal activation (Kakuda et al., 1996, 1998; Gandevia et al., 1997).

In this chapter I will argue that the data of Stuart's group on muscle velocities in gait of different speeds, when combined with a quantitative analysis of the components of spindle Ia response due to velocity, displacement and α–γ coactivation, show that the differences between the

*Corresponding author. Tel.: 1 780 492 3783; Fax 780 492 1617; e-mail: arthur.prochazka@ualberta.ca

firing rates of animal and human spindles may indeed be due mainly to differences in the velocities of movement studied. I arrived at this conclusion with the help of simple mathematical models of spindle response properties. These models are now very easy to realise and manipulate with graphics-based software. An important aim of this chapter is therefore to present a set of models of proprioceptive transduction in this format. The models are reasonably accurate, and yet simple enough to be incorporated into larger models of sensorimotor function. They may be downloaded via the Internet (see later).

Models of spindle and tendon organ transduction

In two recent papers, Monica Gorassini and I tested several models in the literature of the responses of cat spindle (group Ia and II) and tendon organ (group Ib) afferents. We evaluated the accuracy of the various models in predicting the averaged firing profiles of ensembles of single afferents in the step cycle recorded with microwires implanted in the dorsal root ganglia of normal cats (Prochazka and Gorassini, 1998a, b). To our surprise, all of the Ia models, which included those of Matthews and Stein (1969), Chen and Poppele (1978), Houk et al. (1981) and Hasan (1983), fitted the chronic data well, with r^2 values ranging from 0.4 to 0.94. In retrospect, this is not too surprising, because peak muscle velocities are high in the step cycle and as all of the models have a velocity component, this dominated in a similar way in all the predictions. However, when we tested the same models, with the same gain parameters, on Ia responses to slow ramp-and-hold stretches derived from the literature, some predicted the responses better than others (Fig. 1). The most general and accurate model overall was a variant of those proposed by Houk et al. (1981) and Hasan (1983), namely:

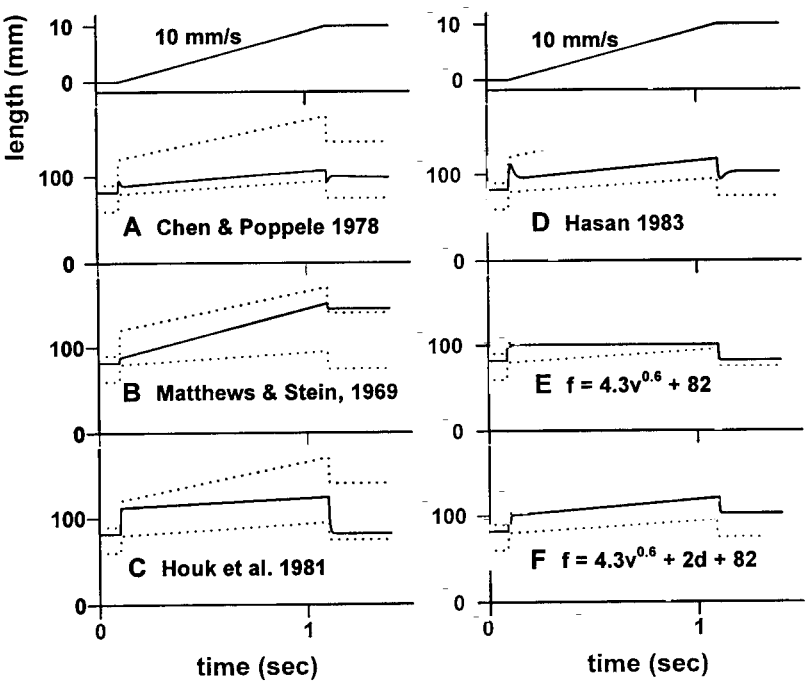

Fig. 1. Predictions of the models of spindle primary responses to ramp-and-hold stretches at a low velocity (10 mm/sec). Dotted lines show the range of spindle primary responses under moderate static fusimotor drive, estimated from the literature. Models without length-sensitive terms (e.g. C and E) did not reproduce the ramp increase in firing rate during stretch, so cannot be considered general. The responses in D and F fall in the middle of the expected range and have appropriate step and ramp components, indicating that their velocity and positional sensitivities are correctly scaled. Reproduced with permission, (Prochazka and Gorassini, 1998a).

$$\text{Ia firing rate} = 4.3*\text{velocity}^{0.6} + 2*\text{displacement} + K\%*\text{EMG} + \text{mean rate} \quad (1)$$

(rate: impulses/s, muscle velocity: mm/s, displacement: mm). The EMG term adds a component of Ia firing proportional to α-motoneuronal activity, representing α-linked γ_{static} action. EMG is the normalized, high-pass-filtered, averaged, rectified EMG of the receptor-bearing muscle, the high-pass transfer function being $(s+1)/(s+20)$. K% is the percentage of maximal EMG recruitment possible in the muscle. Figure 2 shows the EMG term and the overall fit achieved with Equation 1 of the mean firing rate profile of nine hamstrings Ia afferents in the cat step cycle with K% set to 50. The mean rate in the chronic data was 80 impulses/s.

I will now propose a slightly simpler and more general version of the above model, namely:

$$\text{Ia firing rate} = 65*\text{velocity}^{0.5} + 200*\text{displacement} + K\%*\text{EMG} + \text{mean rate} \quad (2)$$

In this case displacement and velocity are expressed in rest lengths (RL and RL/s), and velocity$^{0.5}$ replaces the velocity$^{0.6}$ term in Equation 1. Note that the Ia models as they stand in Equations 1 and 2 cannot be used for negative velocities. We dealt with this by computing the Ia response to the absolute value of velocity and then restoring the sign (see Fig. 5). Although the fits obtained with Equation 1 of the chronically recorded spindle data were slightly better than those with Equation 2, this is offset by the advantage of being able to estimate the square root of velocity easily by mental arithmetic. For example, consider the data of Fig. 2. During the swing phase of the step, hamstrings muscle length

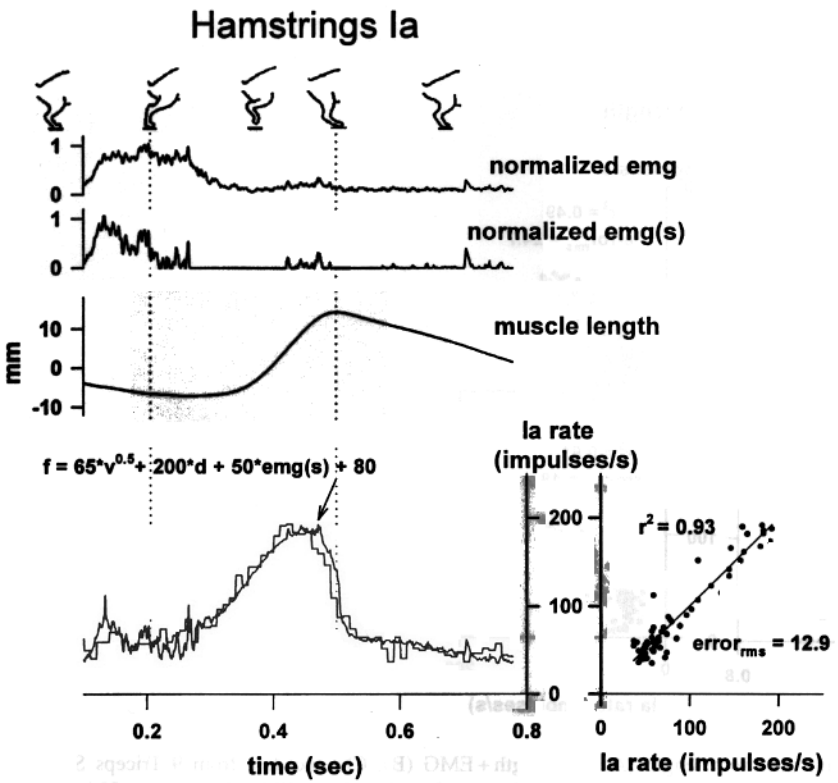

Fig. 2. Prediction of hamstrings Ia firing rate from length and EMG. 9 hamstrings Ia afferents each contributed 4 step cycles of data to the firing rate probability density function. The prediction of Ia rate was computed using Equation 2. The mean rate of the chronic data was 80 impulses/s. The plot at bottom right is of predicted Ia rates (y-axis) versus chronically recorded Ia rates (x-axis). The RMS error was 12.9 impulses/s, i.e. < 8% of modulation depth.

increased 15 mm in about 0.05 s, i.e. velocity was 15/0.05 = 300 mm/s. The rest length of hamstrings is about 100 mm, so 300 mm/s represents 3 RL/s. Equation 2 tells us that the component of Ia firing rate due to this velocity is 65*sqrt3 = 92 impulses/s. Add to this the displacement term 200*0.15 = 30 and a mean rate of 80 from the chronic data and we have a predicted peak firing rate of 202 impulses/s, which agrees well with the peak of the firing rate profile in Fig. 2. From Fig. 3, triceps surae stretches more slowly: ~10 mm in 0.1s during the swing phase, i.e. 0.1 RL in 0.1 s = 1 RL/s. The mean rate of triceps Ia's in our data was 50 impulses/s. Equation 2 thus predicts a peak firing rate of 65 + 20 + 50 = 135 impulses/s. Just before foot touchdown, muscle velocity reverses from +1 to −1 RL/s, leading to a predicted reduction of 2*65 = 130 impulses/s. It is here that the EMG component, representing α-linked γ_{static} action, became very significant in improving the fit of the triceps surae Ia data (compare Fig. 3A and 3B). But even with the EMG-linked term, the fit in B was not as good as that for hamstrings Ia rate profiles (Fig. 2), possibly because of muscle unloading and

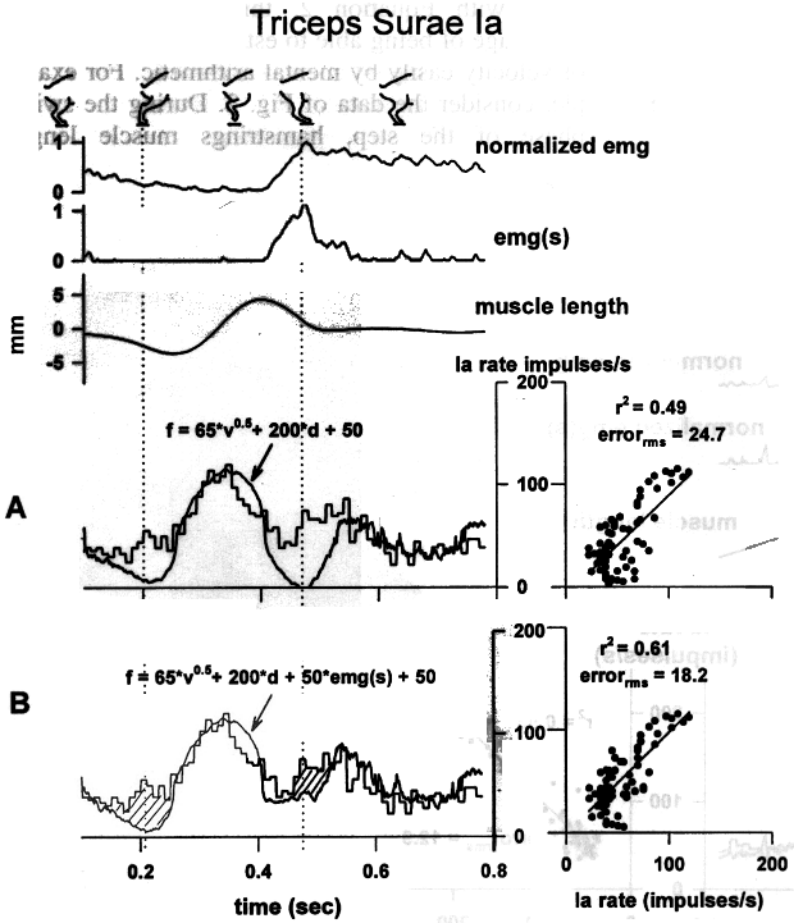

Fig. 3. Prediction of Triceps Surae Ia firing rate from length (A) and length + EMG (B). Chronic data from 9 Triceps Surae Ia afferents, each contributing 4 step cycles. Equation 2 was used to predict Ia firing rate from length and EMG. Mean rate = 50 impulses/s. In A, the EMG component of Equation 2 was set to zero. In B, adding this component (to simulate α-linked fusimotor action) improved the fit (compare B to A), but even then the fit was not as good as that in Fig. 3. This may be due to a discrepancy in origin-to-insertion muscle displacement and the internal displacement 'seen' by the spindles (see text). This Figure is based on the same chronic data as in Fig. 2 of Prochazka et al. (1998b), though with a different set of step cycles.

tendon strain effects in triceps surae, which are maximal just before and after the swing phase respectively: see the shaded portions of Fig. 3B (Hoffer et al., 1989; Elek et al., 1990; Griffiths, 1991). As we will see below, the relative sizes of the velocity and EMG terms are important in resolving some of the differences in Ia firing behavior in cats and humans.

Unfortunately, the firing of group II spindle afferents has rarely been recorded chronically in any species. Monica Gorassini and I only had access to averaged step-cycle profiles from three such afferents. Two were fitted best by a model in which muscle displacement (measured in mm) and normalized, averaged, rectified EMG (non-filtered) were the modulating terms:

$$\text{II firing rate} = 13.5*\text{displacement} + 20*\text{EMG} + \text{mean rate} \quad (3)$$

The third profile was best fitted by filtering the displacement (again in mm) with the Poppele and Bowman group II transfer function and additional EMG_{norm} and mean rate terms:

$$\text{II firing rate} = 0.4*\text{displacement}*(s+0.4)(s+11)/(s+0.8) + 20*\text{EMG} + \text{mean rate} \quad (4)$$

The Poppele and Bowman transfer function is likely to be more general as it not only fitted two of the chronic profiles but was originally based on data obtained in acute experiments, so the recommendation to modellers at this stage is to use Equation 4 with a mean rate of 80 impulses/s to describe group II responses. The EMG term representing α-linked γ_{static} action, has a smaller gain constant than for Ia afferents and this is in line with the conclusion of Loeb and Duysens (1979) and Loeb and Hoffer (1985), that spindle secondaries are modulated largely by muscle length changes. The more general form of (4), in which displacement is expressed in RL is:

$$\text{II firing rate} = 40*\text{displacement}*(s+0.4)(s+11)/(s+0.8) + 20*\text{EMG} + \text{mean rate} \quad (5)$$

Finally, for tendon organ Ib afferents, we used the inverse of the Houk and Simon (1967) model to estimate triceps surae force from the Ib ensemble profile.

Houk and Simon model

$$\text{Ib firing rate} = K*\text{Force}*(s+0.15)(s+.5)(s+16)/(s+0.2)(s+2)(s+37) \quad (6)$$

Inverse

$$\text{Force} = K^{-1}*(\text{Ib firing rate})*(s+0.2)(s+2)(s+37)/(s+0.15)(s+1.5)(s+16) \quad (7)$$

The estimated force profile agreed well with the mean soleus force profile measured with implanted buckle transducers by Fowler et al. (1993) and Herzog et al. (1993) in freely-moving cats (Fig. 4). This indicates that if the time course of force is known (either as a measurement or as a signal computed within a biomechanical model), the ensemble Ib firing profile can be estimated with Equation 6.

The value of the gain constant K depends on whether one uses the force of a single muscle such as soleus or that of a muscle group such as the triceps surae. To simplify matters, normalized force profiles may be used and K then becomes the scale factor that produces appropriate peak Ib firing rates. The value of K^{-1} used in Equation 6 to obtain normalized force from Ib firing rate in Fig. 4 was 0.003. So the recommendation to compute Ib firing rate from normalized force is $K = 333$.

Typically peak soleus force in the stance phase of the cat step cycle is ~20 N (Herzog et al., 1993) and in the whole triceps surae it is ~36 N (Fowler et al., 1993). Among other things this shows that members of a synergistic group do not contribute equal forces. Furthermore, Ib firing rate may not be linearly related to whole muscle force, especially when force is large (Proske, 1981; Crago et al., 1982; Jami, 1992). For example, Walmsley et al. (1978) showed that soleus force ranges from 20 N in gait to 100 N in sudden jumps. Figure 4 shows that peak Ib rate is already over 120 impulses/sec in gait. As it is unlikely that Ib firing rates ever exceed 500–600 impulses/s (personal observations) this implies a saturation in the force-rate relationship. For these reasons and the fact that our tests of analytical models on chronic Ib data are the only ones in the literature so far, any prediction of Ib

responses in normal motor tasks based on Equation 6 should be viewed as approximate only.

If force is unavailable a very rough estimate of Ib firing rate may be obtained from the normalized

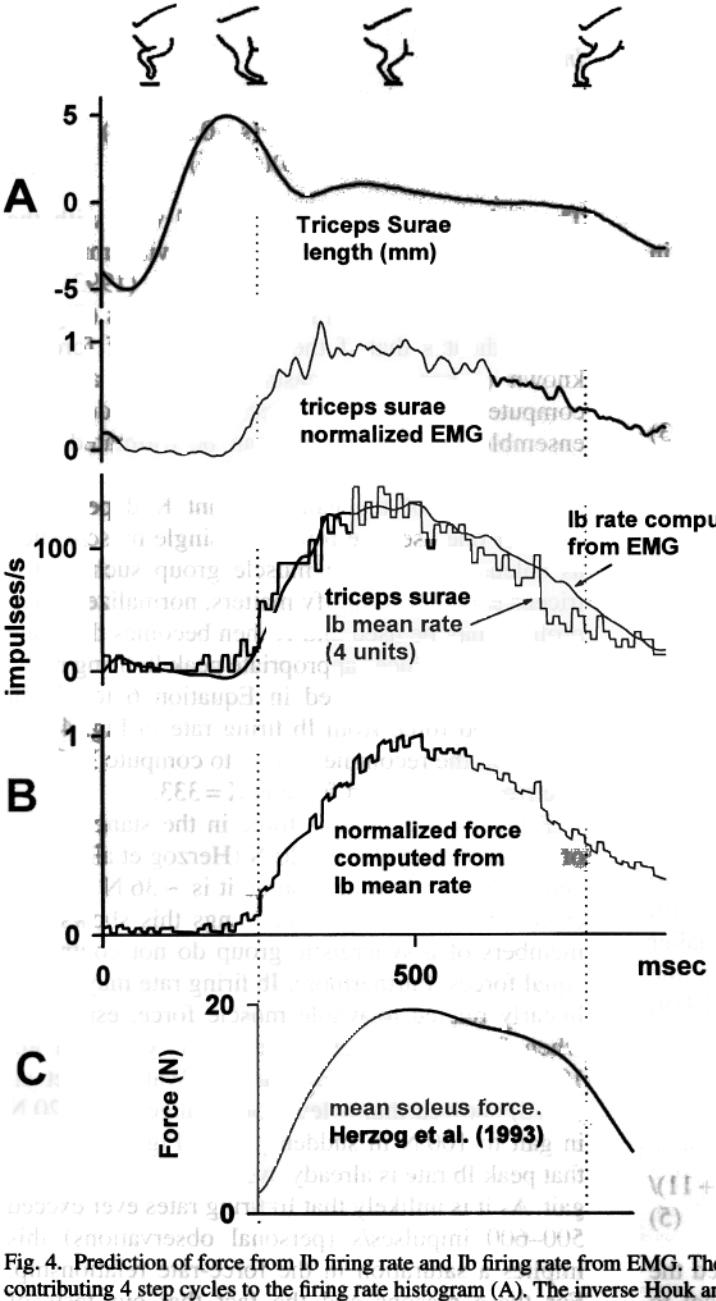

Fig. 4. Prediction of force from Ib firing rate and Ib firing rate from EMG. The chronic data were obtained from four Ib afferents each contributing 4 step cycles to the firing rate histogram (A). The inverse Houk and Simon model of Equation 7 was used to predict force from this firing rate profile (B). Compare B with C, the mean soleus force profile recorded with implanted buckle transducers. Equation 8 was used to predict Ib firing rate from the EMG profile and the result is the smooth superimposed curve in A. This is a modified version of Fig. 7 in Prochazka and Gorassini, 1998b.

EMG by adding some low-pass filtering to Equation 6 (Jacks et al., 1988) and adjusting the gain constant accordingly:

$$\text{Ib firing rate} = 4500*\text{EMG}*(s+0.15)(s+1.5)(s+16)/(s+0.2)(s+(2)(s+37)(s+12) \quad (8)$$

Again it should be understood that EMG is only proportional to muscle force in isometric contractions. Whenever muscles lengthen or shorten appreciably the relationship starts to become nonlinear and the prediction less reliable.

Object-oriented models. For the convenience of the reader, Equations 2, 5, 7 and 8 are implemented in a form suitable for use with Matlab Simulink in Fig. 5. As mentioned above, in the Ia model responses to negative velocities are dealt with by computing the response to the absolute magnitude of velocity and then restoring the sign.

Implications of the models for differences in animal and human spindle firing behavior. Equation 2 tells us that muscle spindle Ia responses are a function of muscle velocity, displacement and α-linked γ action. It is very interesting to compare the data of Douglas Stuart and his colleagues on the ranges of muscle velocity encountered in cat gait with the ranges of velocity that occur in normal human movement and in human neurography experiments. What emerges goes a long way towards explaining the puzzling differences between the animal and human spindle data over the last few years.

In the cat the changes in muscle velocity within each locomotor cycle range from 0.8 to 2.8 RL/s in walking and from 1.2 to 10.0 RL/s in running (Goslow et al., 1973). In human gait, the corresponding values are 0.4 to 0.6 RL/s for walk and 2.0 to 3.0 RL/s for run (derived from Winter, 1987, assuming the full range of motion about a joint corresponds to 0.3 RL change in muscle length). In human neurography experiments since 1967, I have estimated that muscles velocities have ranged from 0 RL/s to 0.1 RL/s (Prochazka, 1981; Prochazka and Hulliger, 1998). If we now use Equation 2 to calculate the mean modulation depth of Ia firing corresponding to the mean changes in velocity, displacement and EMG (representing α-linked γ action), we obtain:

$$\text{Ia firing rate} = 65*\text{velocity}^{0.5} + 200*\text{displacement} + K\%*\text{EMG(s)} \quad (9)$$

cat walk:	87	+	20	+	50
cat run:	154	+	30	+	100
human walk:	46	+	40	+	50
human run:	102	+	60	+	100
neurography:	15	+	20	+	50

In all but the human neurography situation, the estimated modulation of Ia firing due to velocity and displacement combined exceeds that due to α-linked γ action. The slowness of movement in human neurography explains why α–γ linkage has been so prominent a factor. Conversely, Ia firing recorded in freely moving animals emphasizes velocity and displacement rather than α–γ linkage except in strong, relatively isometric contractions. The figures above show that the same would probably hold true if it were possible to record from spindles in human walking and running, though α-linked γ action might be a little more prominent in humans, because muscle velocities (in RL/s) in comparable movements are lower than those in cats. The main point of all this is that the spindle models presented in this article provide a convenient means of estimating the contribution of the different modulating factors and help explain some of the differences in the human and animal data.

Conclusion

Neuromechanical modeling. The above models, along with models of load-moving behavior of muscle can be very useful in testing specific hypotheses. For example, we recently asked how it could possibly be that the reflex excitation of homonymous muscles by tendon organ input during locomotion, which represents positive force feedback, does not completely destabilize the limbs. The result, that the gain of the positive force feedback declines to stable levels as muscles shorten, was as unexpected as it was illuminating (Prochazka et al., 1997). Analytical models of spindle and tendon organ feedback similar to those above were decisive in reaching this conclusion and thanks to object-oriented software and the Internet, the models are readily available to all researchers

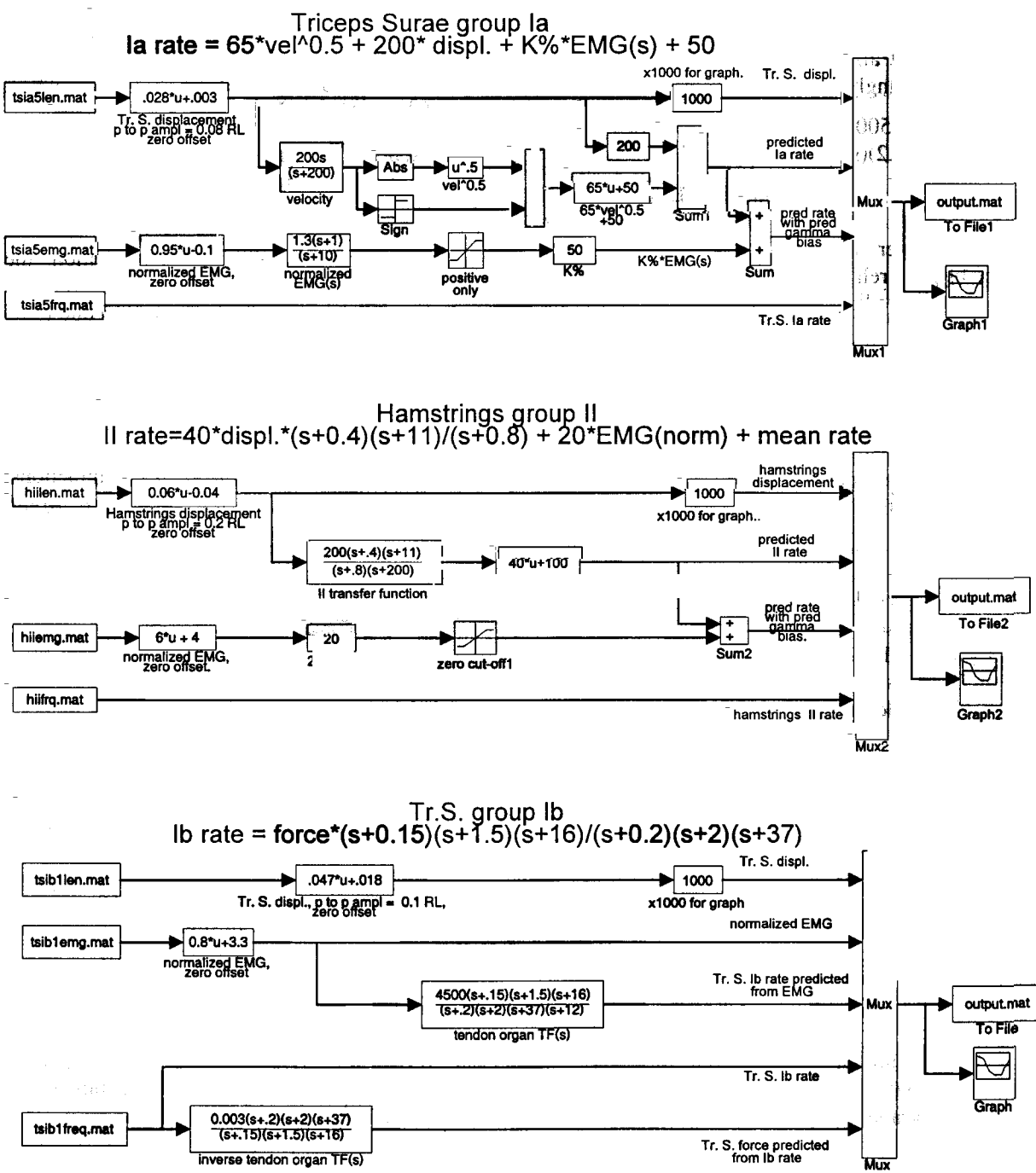

Fig. 5. Object-oriented implementation of Equations 2,5,7 and 8. These are included for the convenience of modellers who use Matlab Simulink software. The boxes at left represent the length, EMG and firing rate profiles stored as Matlab data files. The models and data files in this figure may be downloaded from the following website: http://www.ualberta.ca/~aprochaz/hpage.html.

and can be used and altered with great ease (see Fig. 5 and http://www.ualberta.ca/~aprochaz/hpage.html.). Other control systems approaches to the peripheral control of movement, including finite state control, fuzzy logic and neural networks (Prochazka, 1996) will all depend on core models of sensory feedback such as those described above. Douglas Stuart's vision of moving the field forward by studying neural responses in relation to normal movement is now more relevant than ever.

Acknowledgements

This work was supported by the Canadian Medical Research Council, Neuroscience Canada Foundation, Alberta Paraplegic Foundation and Alberta Heritage Foundation for Medical Research.

References

Chen, W.J. and Poppele, R.E. (1978) Small-signal analysis of response of mammalian muscle spindles with fusimotor stimulation and a comparison with large-signal properties. *J. Neurophysiol.*, 41: 15–27.

Crago, P.E. Houk, J.C. and Rymer, W.Z. (1982) Sampling of total muscle force by tendon organs. *J. Neurophysiol.*, 47: 1069–1083.

Elek, J., Prochazka, A., Hulliger, M. and Vincent, J. (1990) In-series compliance of gastrocnemius muscle in cat step cycle: do spindles signal origin-to-insertion length? *J. Physiol.*, 429: 237–258.

Evarts, E.V. (1964) Temporal patterns of discharge of pyramidal tract neurons during sleep and waking in the monkey. *J. Neurophysiol.*, 27: 152–171.

Fowler, E.G., Gregor, R.J., Hodgson, J.A. and Roy, R.R. (1993) Relationship between ankle muscle and joint kinetics during the stance phase of locomotion in the cat, *J. Biomech.*, 26: 465–483.

Gandevia SC. Wilson LR. Inglis JT. Burke D. (1997) Mental rehearsal of motor tasks recruits α-motoneurones but fails to recruit human fusimotor neurones selectively. *J. Physiol.*, 505: 259–66.

Goslow, G.E. Reinking, R.M. and Stuart, D.G. (1973a) The cat step cycle: hind limb joint angles and muscle lengths during unrestrained locomotion. *J. Morphol.*, 141: 1–42.

Goslow, G.E. Stauffer, E.K. Nemeth, W.C. and Stuart, D.G. (1973b) The cat step cycle: responses of muscle spindles and tendon organs to passive stretch within the locomotor range. *Brain Res.*, 60: 35–54.

Griffiths, R.I. (1991) Shortening of muscle fibres during stretch of the active cat medial gastrocnemius muscle: The role of tendon compliance. *J. Physiol.*, 436: 219–236.

Hagbarth, K.-E. and Vallbo, A.B. (1967) Afferent response to mechanical stimulation of muscle receptors in man. *Acta. Soc. Med. Upsalien*, 72: 102–104.

Hasan, Z. (1983) A model of spindle afferent response to muscle stretch. *J. Neurophysiol.*, 49: 989–1006.

Herzog, W., Leonard, T.R. and Guimaraes, A.C. (1993) Forces in gastrocnemius, soleus, and plantaris tendons of the freely moving cat. *J. Biomech.*, 26: 945–953.

Hoffer, J.A. Caputi, A.A. Pose, I.E. and Griffiths, R.I. (1989) Roles of muscle activity and load on the relationship between muscle spindle length and whole muscle length in the freely walking cat. In: J.H.J. Allum and M. Hulliger (Eds), *Afferent Control of Posture and Locomotion, Progress in Brain Res.* Vol. 80, Elsevier, New York, pp. 75–85.

Houk, J.C. Rymer, W.Z. and Crago, P.E. (1981) Dependence of dynamic response of spindle receptors on muscle length and velocity. *J. Neurophysiol.*, 46: 143–166.

Houk, J.C. and Simon, W. (1967) Responses of Golgi tendon organs to forces applied to muscle tendon. *J. Neurophysiol.*, 30: 1466–1481.

Jacks, A., Prochazka, A. and Trend, P.St.J. (1988) Instability in human forearm movements studied with feedback-controlled electrical stimulation of muscles. *J. Physiol.*, 402: 443–461.

Jami, L. (1992) Golgi tendon organs in mammalian skeletal muscle: functional properties and central actions. *Physiol. Rev.*, 72: 623–666.

Jasper, H. Ricci G.F. and Doane, B. (1958) Patterns of cortical neurone discharge during conditioned responses in monkeys. In: G. Wolstenholme and C. O'Connor (Eds), *Neurological Basis of Behavior*, Boston: Little Brown.

Kakuda, N. and Nagaoka, M. (1998) Dynamic responses of human spindle afferents to stretch during voluntary contractions. *J. Physiol.*, 513: 621–628.

Kakuda, N., Vallbo A.B. and Wessberg J. (1996) Fusimotor and skeletomotor activities are increased with precision finger movement in man. *J. Physiol.*, 492: 921–929.

Loeb, G.E., Bak, M.J. and Duysens, J. (1977) Long-term unit recording from somatosensory neurons in the spinal ganglia of the freely walking cat. *Science*, 197: 1192–1194.

Loeb, G.E. and Duysens, J. (1979) Activity patterns in individual hindlimb primary and secondary muscle spindle afferents during normal movements in unrestrained cats. *J. Neurophysiol.*, 42: 420–440.

Loeb, G.E. and Hoffer, J.A. (1985) Activity of spindle afferents from cat anterior thigh muscles. II. Effects of fusimotor blockade. *J. Neurophysiol.*, 54: 565–577.

Matthews, P.B.C. and Stein, R.B. (1969) The sensitivity of muscle spindle afferents to small sinusoidal changes of length. *J. Physiol.*, 200: 723–743.

Prochazka, A. (1981) Muscle spindle function during normal movement. In: R. Porter (Ed.), *International Review Physiol.*, 25, (Neurophysiol. IV), University Park Press, Baltimore, pp. 47–90.

Prochazka, A. (1996) Proprioceptive feedback and movement regulation. In: L. Rowell and T. Sheperd (Eds), *Handbook of Physiology. Section 12. Exercise: Regulation and Integration of Multiple Systems*, American Physiological Society, New York, pp. 89–127.

Prochazka, A., Gillard, D. and Bennett, D.J. (1997) Implications of positive force feedback in the control of movement. *J. Neurophysiol.*, 77: 3237–3251.

Prochazka, A and Gorassini, M. (1998a) Ensemble firing of muscle afferents recorded during normal locomotion in cats. *J. Physiol.*, 507: 277–291.

Prochazka, A and Gorassini, M. (1998b) Models of ensemble firing of muscle afferents recorded during normal locomotion in cats. *J. Physiol.*, 507: 293–304.

Prochazka, A. and Hulliger, M. (1998) The continuing debate about CNS control of proprioception *J. Physiol.*, 513.2: 315.

Prochazka, A., Westerman, R.A. and Ziccone, S. (1976) Discharges of single hindlimb afferents in the freely moving cat. *J. Neurophysiol.*, 39: 1090–1104.

Proske, U. (1981) The Golgi tendon organ: properties of the receptor and reflex action of impulses arising from tendon organs. In: R. Porter (Ed.), *International Review Physiol.*, 25, (Neurophysiol. IV), University Park Press, Baltimore, pp. 127–171.

Rasmussen, S., Chan, A.K. and Goslow, G.E. (1978) The cat step cycle: electromyographic patterns for hindlimb muscles during posture and unrestrained locomotion. *J. Morphol.*, 155: 253–270.

Walmsley, B. Hodgson, J.A. and Burke, R.E. (1978) Forces produced by medial gastrocnemius and soleus muscles during locomotion in freely moving cats. *J. Neurophysiol.*, 41: 1203–1216.

Wetzel, M.C. and Stuart, D.G. (1976) Ensemble characteristics of cat locomotion and its neural control. *Prog. Neurobiol.*, 7: 1–98.

Winter, D.A. (1987) *The Biomechanics and Motor Control of Human Gait*. University of Waterloo Press, Waterloo Canada, p. 72.